SRT2183 and SRT1720, but not Resveratrol, Inhibit Osteoclast Formation and Resorption in the Presence or Absence of Sirt1

Ramkumar Thiyagarajan
University at Buffalo - The State University of New York
Maria Rodríguez-Gonzalez
University at Buffalo - The State University of New York
Catherine Zaw
University at Buffalo - The State University of New York
Kenneth Ladd Seldeen
University at Buffalo - The State University of New York
Mireya Hernandez
University at Buffalo - The State University of New York
Manhui Pang
University at Buffalo - The State University of New York
Bruce Robert Troen (troen@buffalo.edu)
University at Buffalo - The State University of New York https://orcid.org/0000-0002-3699-0021

Research article

Keywords: osteoporosis, Sirt1, OC-Sirt1KO, osteoclasts, actin belts, bone resorption, bone marrow cells

Posted Date: December 11th, 2020

DOI: https://doi.org/10.21203/rs.3.rs-125262/v1

Abstract

Background: Osteoclastic bone resorption markedly increases with aging, leading to osteoporosis characterized by weak and fragile bones. Mice exhibit greater bone resorption and poor bone mass when Sirt1 is removed from their osteoclasts. Here we investigated the *ex vivo* impacts of putative Sirt1 activators, resveratrol (RSV), SRT2183 and SRT1720, on osteoclast formation and activity in primary mouse bone marrow cells (BMCs) derived from wild type (WT) and osteoclast specific Sirt1 knockout (OC-Sirt1KO) mice and in the RAW264.7 mouse macrophage cell line.

Results: We found that SRT2183 and SRT1720 inhibit formation of osteoclasts and actin belts in both BMCs and RAW264.7 cells, whereas RSV does not. We also observed that the OC-Sirt1KO mice exhibited less bone mineral density, and the BMCs harvested from these mice yielded more osteoclasts than BMCs harvested from littermate controls. Interestingly, both SRT2183 and SRT1720 reduced osteoclast and actin belt formation in BMCs from OC-Sirt1KO mice. SRT2183 and SRT1720 also significantly disrupted actin belts of mature osteoclasts from WT mice BMCs, within 3 and 6 hours of administration. Furthermore, these compounds inhibited resorption activity of mature osteoclasts, while RSV did not.

Conclusion: Our findings suggest SRT2183 and SRT1720 impede bone resorption by disrupting actin belts of mature osteoclasts, inhibit actin belt formation, and inhibit osteoclastogenesis even in the absence of Sirt1. Thus, further understanding the mechanism of action of these compounds may pave the way for potential new therapies in alleviating osteoporosis associated bone loss.

1.0 Introduction

More than half of Americans over age 50 will be at risk for an osteoporosis associated fracture, a leading cause of morbidity and mortality in older individuals. Sirtuin (Sirt1), a nicotinamide adenine dinucleotide dependent deacetylase, is known to increase the healthspan and lifespan and delay the onset of many aging-related diseases in mice (Howitz et al., 2003; Rogina and Helfand, 2004; Wood et al., 2004; Baur et al., 2006; Dali-Youcef et al., 2007; Banks et al., 2008; Satoh et al., 2013; Mercken et al., 2014; Mitchell et al., 2014), and also appears to increase bone mass (Zainabadi et al., 2017). Young mice without Sirt1 in their osteoclasts exhibit greater bone resorption and diminished bone mineral density (BMD) (Edwards et al., 2013; Zainabadi et al., 2017).

Resveratrol (RSV), a natural polyphenol/phytoalexin, increases Sirt1 expression and life span in yeast, C. elegans, and drosophila (Howitz et al., 2003; Rogina and Helfand, 2004; Wood et al., 2004). Mice treated with RSV exhibit greater bone mineral density, bone strength, and trabecular thickness (Pearson et al., 2008). In addition, RSV treated osteoporotic rats show increased bone mineral density and bone strength, as well as reduced femoral porosity as compared to untreated osteoporotic counterparts (Wang et al., 2017). SRT1720 and SRT2183 are structurally different from RSV, but were designed specifically to activate Sirt1, and both compounds exert impacts on bone metabolism (Milne et al., 2007; Gurt et al., 2015; Zainabadi et al., 2017). Treatment of middleaged male mice and young ovariectomized female

mice with SRT1720 increases bone volume (Zainabadi et al., 2017). Further, Gurt et al., showed that *ex vivo* treatment of bone marrow cells (BMCs), from 8-week-old female 129/Sv mice, with SRT2183 inhibits osteoclast formation and diminishes bone resorption activity, and used constitutive Sirt1 knockout mice (lacking Sirt1 exons 5, 6 and 7) to demonstrate the role of Sirt1 on osteoclastogenesis (Gurt et al., 2015).

However, the mode of action of these compounds remains poorly elucidated, and previous studies involving various biochemical assays and biophysical tests have revealed that RSV, SRT2183 and SRT1720 act on targets other than Sirt1 (Huber et al., 2010; Pacholec et al., 2010). Thus, we investigated the impact of RSV, SRT2183, and SRT1720 upon osteoclast formation and resorption in BMCs from skeletally mature (4 month old C57BL/6) male WT. In addition, in order to test to impact of Sirt1 in osteoclast formation, we created a mouse model that lacks the Sirt1 catalytic domain (exon 4) $Sirt1^{exon4-/-}$ specifically in osteoclast precursors (Edwards et al., 2013). We have found that SRT2183 and SRT1720 consistently inhibit osteoclastogenesis and actin belt formation independent of the presence of intact Sirt1. Furthermore, SRT2183 and SRT1720 significantly disrupt actin belts and inhibit resorption activity of mature osteoclasts.

2.0 Methods

2.1 Mice

All studies and experimental protocols were approved by and were in compliance with guidelines of the Miami VA Animal Care and Use Committee, the University at Buffalo, and the VA Western New York Institutional Animal Care and Use Committees. Male C57BL/6 mice were housed in large animal cages containing 2 or 3 mice per cage and were maintained under a 12hour light and 12hour dark cycle and at all times provided *ad libitum* access to chow and water. The osteoclast specific $Sirt1^{exon4-/-}$ (OC-Sirt1KO) mice were a kind gift from Dr. James Edwards (Edwards et al., 2013), and the mice line was bred and maintained in our facility. In order to maintain the colony, the mice with exon 4 mutation were mated with mice expressing the Cre recombinase specifically in osteoclasts (driven by the lysozyme M promoter). The 4-month-old mice were anesthetized with intraperitoneal injection of ketamine and xylazine (100 mg/kg and 20 mg/kg mouse, respectively) and then euthanized by cervical dislocation in the animal facility surgical room between 10AM and 12PM.

2.2 Reagents

Resveratrol was purchased from Sigma-Aldrich (St. Louis, MO). SRT1720, and SRT2183 were purchased from Calbiochem (San Diego, CA), and Selleckchem (Houston, TX), respectively. Soluble mouse RANKL was acquired from Santa Cruz Biotechnology (Santa Cruz, CA). Recombinant mouse M-CSF (mM-CSF) was obtained from R&D Systems (Minneapolis, MN). High glucose alpha-MEM (α-MEM), and 100X penicillin G/streptomycin were purchased from Life Technologies/Invitrogen (Grand Island, NY). Fetal Bovine Serum (FBS) was from Thermo Scientific/Hyclone (Logan, UT). All other reagents used in this study were from Sigma-Aldrich.

2.3 Bone mineral density measurement

Bone mineral density (BMD) was measured by dual-energy x-ray absorptiometry (DEXA) using a Lunar PIXImus II (Inside Outside Sales, LLC., Fitchburg, Wisconsin). Fourmonthold WT and OC-Sirt1KO male mice ($n = 6$) were anesthetized with intraperitoneal injection of ketamine and xylazine (100 mg/kg and 20 mg/kg mouse, respectively) and then DEXA analysis was performed as a single scan.

2.4 Primary BMC isolation

BMCs isolated from C57BL/6J mice were used for bone marrow macrophage and osteoclast differentiation. Briefly, BMCs were flushed from tibiae and femorae. After the lysis of red blood cells, the BMCs were plated in a 10 cm tissue culture dish with α-MEM complete medium (basal α-MEM medium supplemented with 10% FBS, 100 U/ml penicillin G, and 100 μg/ml streptomycin and 2 mM glutamine) and 20 ng/ml mM-CSF (macrophage/monocyte colony stimulating factor). After an overnight incubation in a humidified atmosphere of 5% CO_2 at 37 °C, the non-adherent BMCs were collected for further experimentation.

2.5 RAW264.7 cell culture

RAW264.7 cells were purchased from American Type Culture Collection (ATCC, Manassas, VA). The RAW264.7 cells were maintained in high glucose D-MEM complete medium (basal D-MEM supplemented with 10% fetal bovine serum, 100 U/ml penicillin G, and 100 μg/ml streptomycin and 2 mM glutamine), and in a humidified atmosphere of 5% CO_2 at 37 °C. Cells were maintained in suspension culture in non-coated petri dishes (Greiner Bio-one, Monroe, NC), which markedly reduces drift toward a differentiated state. For experiments cells were plated on standard tissue culture dishes.

2.6 Cell viability assay

After overnight incubation with 20 ng/ml mM-CSF, the non-adherent BMCs were collected and plated as 1×10^5 cells/0.25 ml/well in a 96 well plate with 20 ng/ml mM-CSF and 40 ng/ml RANKL in the presence or absence of RSV, SRT2183 and SRT1720 for 3 days. Similarly, RAW264.7 cells plated as 1000 cells/0.25 ml/well in a 96 well plate with 40 ng/ml RANKL in the presence or absence of RSV, SRT2183 and SRT1720 for 3 days. After 3 days, cell viability was assessed using Vybrant® MTT Cell Proliferation Assay Kit, (Thermo Fischer Scientific, Grand Island, NY) following the manufacturer's protocol. Briefly, 12 mM MTT (3-(4,5-dimethylthiazol-2-yl)-2,5-diphenyltetrazolium bromide) is added to the cells, which is then converted to insoluble formazan. The insoluble formazan was solubilized using SDS-HCl solution, and the concentration determined by optical density at 570 nm.

2.7 Osteoclast differentiation and visualization of osteoclasts and actin belts

The non-adherent cells were resuspended in αMEM complete medium, containing 20 ng/ml mM-CSF and 40 ng/ml RANKL, and subsequently cultured in 24-well plates at a density of 5×10^5 cells per well, in the

presence or absence of RSV, SRT2183 and SRT1720. Medium was replaced every 23 days with fresh mMCSF and RANKL for 6–7 days. The RAW264.7 cells were cultured in a 48 well plate at a density of 4×10^3 per well and were differentiated with 40 ng/ml of RANKL in α-MEM complete medium for 3–4 days. The differentiated osteoclasts were fixed and stained either with tartrate resistance acid phosphatase (TRAP) kit (Sigma-Aldrich) to visualize osteoclasts or FITC-phallodin to visualize actin belts. The TRAP-positive multinucleated osteoclasts (≥ 3 nuclei) were counted manually.

2.8 Disruption of actin belts of mature osteoclasts

After 6–7 days of differentiation of BMCs or 3–4 days of differentiation of RAW264.7 to osteoclasts, the mature osteoclasts were treated with vehicle (0.1% DMSO), RSV, SRT2183, or SRT1720 for 3 and 6 hours. After the 3 or 6 hour time points, the actin belts of mature osteoclasts were fixed and visualized with FITC-phalloidin.

2.9 Resorption pit assay on cortical bovine bone slices

On day 7, mature osteoclasts were lifted off the plate, using accutase solution (Sigma-Aldrich) and reseeded on cortical bovine bone slices (Boneslices.com, Jelling, Denmark) at a density of 5×10^4 cells per bone slice (6 mm diameter and 0.4 mm thickness) in a 96 well plate. The osteoclasts were cultured in α-MEM complete media, containing 20 ng/ml mM-CSF, 40 ng/ml RANKL and with or without RSV, SRT2183 and SRT1720. After 3 days the cells were removed using cotton swabs and the resorption pits were visualized with 0.1% toluidine blue and quantified with ImageJ software (Schneider et al., 2012).

2.10 Cell lysate preparation and western blotting

Following various treatments, BMCs or osteoclasts were washed with cold PBS and lysed in cold RIPA buffer. Lysates were kept on ice and vortexed for 15 seconds, every 10 min, three times. Cell lysates were centrifuged at 17,000 g for 15 min at 4°C, and the supernatants were collected. Pierce bicinchoninic acid (BCA) protein assay solution (Thermo Fischer Scientific, Grand Island, NY) was added to supernatants and protein standards, and then the protein concentration was measured using a standard plate reader (Bio-Rad Laboratories Ltd., Hercules, CA) at 560 nm. Approximately 30 µg of protein were separated on a 8% SDS-PAGE and electro-transferred to a PVDF membrane. Membranes were blocked in 5% milk in tris-buffered saline with 0.05% Tween 20 for 1 hour at room temperature, and then incubated overnight with anti-Sirt1 antibody (07–131, Millipore, Burlington, MA) or anti-AMPKα (AMP-activated protein kinase-alpha, 2603, Cell Signaling Technology, Danvers, MA) or anti-phosphorylated AMPKα (2535, Cell Signaling Technology, Danvers, MA) at 4°C. The next day, the membrane was washed with TBST and incubated with horseradish peroxidase-conjugated secondary antibody (1:5000) for 1 hour at room temperature. Protein bands were detected by chemiluminescence using Pierce™ ECL western blotting substrate (Thermo Fischer Scientific, Grand Island, NY). GAPDH (ab181602, Abcam, Cambridge, UK) was used as the reference protein.

2.11 Data analysis

Data are expressed as mean ± SD. One-way ANOVA and post hoc Tukey's multiple comparisons test were applied to analyze differences between vehicle control, RSV, SRT2183, and SRT1720 treatments using Graphpad software. Comparisons between WT and Sirt1KO mice were performed using an unpaired Student's T-Test. P-values of < 0.05 were considered statistically significant.

3.0 Results

3.1 SRT2183 and SRT1720 inhibit osteoclast and actin belt formation, while RSV does not

We assessed the viability of the BMCs with various concentrations of the compounds. RSV at 12.5 μM impaired BMC viability by 60% (S1A Fig), whereas in RAW264.7 cells 10 μM RSV reduced cell viability by more than 90% (S1B Fig). Therefore, we used a concentration of 5 μM RSV on both BMCs and RAW264.7 cells.

5 μM RSV did not impede RANKL induced osteoclast formation in primary BMCs (Figs. 1A and 1B) and RAW264.7 cells (S2A and S2B Figs). In contrast to RSV, SRT2183 (5 μM) and SRT1720 (0.6 μM) markedly inhibited the osteoclastogenesis in a dose dependent manner (Figs. 1A and 1B) without affecting viability (S1A and S1B Figs). We further examined whether these compounds altered actin belt formation, which is essential for bone resorption. Both SRT2183 and SRT1720 significantly inhibited actin belt formation in BMCs (Figs. 2A and 2B) and RAW264.7 cells (S2C and S2D Figs), while RSV did not inhibit actin belt formation.

3.2 Osteoclasts specific Sirt1 knockout (OC-Sirt1KO) mice exhibit low bone mineral density

It is reported that Sirt1 plays an important role in osteoclastogenesis (Gurt et al., 2015; Kim et al., 2015; Zainabadi et al., 2017). In order to understand the impact of Sirt1 on bone, we utilized transgenic mice with osteoclast specific ablation of the Sirt1 exon4, which comprises the catalytic domain that confers Sirt1 deacetylase activity (Cheng et al., 2003). We confirmed the truncated Sirt1 protein using immunoblotting (Fig. 3A). The OC-Sirt1KO mice exhibited decreased bone mineral density (BMD: 52.2 ± 0.6 mg/cm^2 versus 55.6 ± 2.7 mg/cm^2, $p < 0.05$) compared to WT littermate controls (Fig. 3B). Further, BMCs harvested from OC-Sirt1KO mice exhibited greater osteoclastogenesis ($p < 0.001$) than did those from the littermate controls (Figs. 3C and 3D).

3.3 SRT2183 and SRT1720 inhibit osteoclast and actin belt formation in BMCs derived from osteoclast specific Sirt1KO (OC-Sirt1KO) mice

We therefore set out to determine whether Sirt1 mediated the impacts of SRT2183 and SRT1720 inhibition of osteoclast formation. Interestingly, both SRT2183 and SRT1720 significantly inhibited osteoclastogenesis in BMCs from the OC-Sirt1KO mice, whereas RSV did not (Figs. 4A and 4B). Furthermore, SRT2183 and SRT1720 markedly suppressed actin belt formation in BMCs harvested from OC-Sirt1KO mice, whereas again RSV did not (Figs. 4C and 4D).

3.4 SRT2183 and SRT1720 disrupt actin belts of mature osteoclasts and prevent bone resorption, while RSV does not

Since actin belts are required for bone resorption by mature osteoclasts and SRT2183 and SRT1720 significantly inhibit actin belt formation and osteoclastogenesis, we therefore set out to assess the impacts of these compounds on mature osteoclasts. We found that both SRT2183 and SRT1720 disrupted actin belts in mature osteoclasts within 3 hours and 6 hours after treatment, respectively (Fig. 5A). Similarly, in RAW264.7 cells, SRT2183 disrupted actin belts at 3 hours, while SRT1720 took 30 hours to completely disrupt actin belts of mature osteoclasts (S3 Fig). We next set out to assess whether the disruption of actin belts of mature osteoclasts by these compounds affected osteoclastic bone resorption. We reseeded mature osteoclasts on bovine cortical bone slices and then treated with RSV, SRT2183 and SRT1720 for 72 hours, to provide sufficient time for resorption. We found that the SRT2183 ($p < 0.001$) and SRT1720 ($p < 0.001$) significantly diminished resorption pits (eroded area) on bone slices, while RSV did not (Figs. 5B and 5C).

4.0 Discussion

During osteoporosis, osteoclastic bone resorption overwhelms bone formation leading to loss of bone mass and increased fragility (Feng and McDonald, 2011). Dynamic bone resorption requires mature osteoclasts with intact actin belts. Here we examined the role of Sirt1 activators (RSV, SRT2183 and SRT1720) on osteoclastic bone resorption, *ex vivo*. We found that SRT2183 and SRT1720 inhibit the formation of osteoclasts and actin belts in primary BMCs derived from both WT and OC-Sirt1KO mice, while RSV does not. We also observed SRT2183 and SRT1720 inhibit bone resorption by disrupting actin belts of mature osteoclasts. Our findings contrast with previous studies that showed reduced osteoclast formation with RSV treatment in various cell types, such as monocytes from human peripheral blood mononuclear cells, primary bone derived cells from canine bone fragments, and RAW264.7 cells (Boissy et al., 2005; He et al., 2010; Shakibaei et al., 2011; Feng et al., 2018). To our knowledge, no previous *ex vivo* studies have shown the effect of RSV on osteoclastogenesis in mouse primary BMCs. We chose a 5 μM concentration of RSV based on our cell viability assay data. To our surprise, 5 μM RSV did not reduce osteoclastogenesis and instead appears to increase osteoclast formation in both BMCs and RAW264.7 cells. In contrast, He et al. showed that 3 μM RSV reduced osteoclastogenesis in RAW264.7 cells (He et al., 2010). We note that although RSV did not inhibit osteoclast and actin belt formation in our

experiments, it increased phosphorylation of AMPKα (S4 Fig) in both BMMs and RAW264.7 cells, which indicates that RSV activated Sirt1, consistent with previous reports (Price et al., 2012; Lan et al., 2017). Thus, the differences between our findings and those of He et al. may be due to the number of RAW264.7 cells plated (20,000 cells versus 12,500 cells per well) and the concentration of RANKL used to differentiate RAW264.7 cells to osteoclasts (40 ng/ml of RANKL versus 3 ng/ml of RANKL) (He et al., 2010).

However, we observed that both SRT2183 and SRT1720 significantly inhibit RANKL induced differentiation of primary BMCs from young male mice and RAW264.7 to osteoclasts. To our knowledge, no studies have tested the *ex vivo* effect of SRT1720 on osteoclastogenesis in primary BMCs. Nevertheless, a recent *in vivo* study by Zainabadi et al., demonstrated that SRT1720 treatment improved bone health in middle-aged male mice and in overiectomized female mice (Zainabadi et al., 2017). Furthermore, consistent with our findings, Gurt et al., observed fewer osteoclasts after treatment of primary BMCs harvested from 8-week-old female 129/Sv mice with 1 uM SRT2183 *ex vivo* (Gurt et al., 2015).

As Sirt1 is known to regulate bone mineral metabolism, we studied osteoclasts generated from BMCs harvested from osteoclast specific Sirt1 knockout (OC-Sirt1KO) mice. We found that OC-Sirt1KO mice exhibited less bone mineral density, and BMCs harvested from these mice yielded more osteoclasts as compared to WT mice. In support of these observations, previous studies have also observed poor bone mass and greater osteoclastogenesis in OC-Sirt1KO mice as compared to the littermate controls (Edwards et al., 2013; Zainabadi et al., 2017). This supports a role for Sirt1 in osteoclastogenesis. Surprisingly, although SRT2183 and SRT1720 are considered as Sirt1 activating compounds (Feige et al., 2008; Smith et al., 2009; Yamazaki et al., 2009), both of these agents inhibited osteoclast and actin belt formation in BMCs harvested from the OC-Sirt1KO male mice. These findings are consistent with the previous study by Gurt et al., showing that SRT2183 inhibits osteoclast formation and resorption activity in BMCs from constitutive Sirt1 knockout female mice (Gurt et al., 2015). In addition, Huber et al., and Pacholec et al., demonstrated Sirt1 independent effects of SRT2183 and SRT1720 on mouse embryonic fibroblasts and human bone osteosarcoma epithelial cells (U2OS), but not on BMCs or osteoclasts (Huber et al., 2010; Pacholec et al., 2010). In contrast, studies have also demonstrated Sirt1-dependent beneficial impacts of these Sirt1 activating compounds (Hubbard et al., 2013; Mercken et al., 2014). Our *in vivo* data shows that Sirt1 may take part in bone mineral metabolism by altering BMD in OC-Sirt1KO mice, but is not required for SRT2183 or SRT1720 to inhibit actin belt organization and osteoclastogenesis *ex vivo*.

Organized actin rings form a stable actin belt in mature osteoclast, which is an important factor for osteoclastic bone resorption. Actin belts generate a sealing zone under which energy consuming dynamic bone resorption occurs (Saltel et al., 2008), and it has been shown that the targeted disruption of genes responsible for actin cytoskeleton organization leads to poor bone resorption (Soriano et al., 1991; Lowe et al., 1993). In our study, SRT2183 and SRT1720 consistently disrupted the actin belts of mature osteoclasts and efficiently inhibited resorption pit formation in cortical bovine bone slices. Gurt et al., also

demonstrated poor pit formation by SRT2183 treated osteoclasts derived from mouse BMCs (Gurt et al., 2015).

5.0 Conclusion

Our results indicate that both SRT2183 and SRT1720 inhibit osteoclast and actin belt formation in primary BMCs harvested from both WT and OC-Sirt1KO mice, while RSV does not. These Sirt1 activating compounds therefore can act independent of Sirt1. Furthermore, SRT2183 and SRT1720 efficiently inhibit bone resorption by disrupting actin belts of mature osteoclasts. These findings support a role for compounds that disrupt actin belts of osteoclasts a potential treatment for osteoporosis.

6.0 List Of Abbreviations

BMC – Bone marrow cell

BMD – Bone mineral density

DMSO – Dimethy sulfoxide

KO – Knock out

OC – Osteoclast

RSV – Resveratrol

Sirt – Sirtuin

WT – wild type

7.0 Declarations

7.1 Ethics approval and consent to participate

All studies and experimental protocols were approved by and were in compliance with guidelines of the Miami VA Animal Care and Use Committee, the University at Buffalo, and the VA Western New York Institutional Animal Care and Use Committees. The osteoclast specific Sirt1$^{exon4-/-}$ (OC-Sirt1KO) mice were a kind gift from Dr. James Edwards

7.2 Consent for publication

Not applicable

7.3 Availability of data and materials

Submitted as a supplementary file in the BMSD editorial manager.

7.4 Competing interests

All authors have no conflicts of interest

7.5 Funding

Supported by VA Merit review (BX000758), NIH (5K07AG06026602), and the Indian Trail Foundation. The funders had no role in study design, data collection and analysis, decision to publish, or preparation of the manuscript

7.6 Author contributions

Conceptualization: MP, RT, KS, BT

Investigation: MR, CZ, MH, RT

Methodology: MP, RT, BT

Supervision: MP, KS, BT

Resources: BT

Writing – original draft: RT

Writing – review & editing: RT, KS, BT

7.7 Acknowledgements

Research supported by Indian Trail Foundation, VA Merit Review (BX000758), NIH (5K07AG06026602), and the Department of Medicine, Jacobs School of Medicine and Biomedical Sciences, University at Buffalo. We thank Dr. Kent Søe, Associate Professor, Clinical Cell Biology, Department of Pathology, Odense University Hospital, University of Southern Denmark, 5000 Odense C, Denmark for providing valuable suggestions on the analysis of resorption pits in bovine bone slices.

8.0 References

1. Office of the surgeon general (us). Bone health and osteoporosis: A report of the surgeon general. Rockville (md): Office of the surgeon general (us); (2004). Available from: Https://www.Ncbi.Nlm.Nih.Gov/books/nbk45513/.
2. Banks, A.S., N. Kon, C. Knight, M. Matsumoto, R. Gutierrez-Juarez, L. Rossetti, W. Gu and D. Accili, 2008. Sirt1 gain of function increases energy efficiency and prevents diabetes in mice. Cell Metab, 8(4): 333-341. Available from http://www.ncbi.nlm.nih.gov/pubmed/18840364. DOI 10.1016/j.cmet.2008.08.014.

3. Baur, J.A., K.J. Pearson, N.L. Price, H.A. Jamieson, C. Lerin, A. Kalra, V.V. Prabhu, J.S. Allard, G. Lopez-Lluch, K. Lewis, P.J. Pistell, S. Poosala, K.G. Becker, O. Boss, D. Gwinn, M. Wang, S. Ramaswamy, K.W. Fishbein, R.G. Spencer, E.G. Lakatta, D. Le Couteur, R.J. Shaw, P. Navas, P. Puigserver, D.K. Ingram, R. de Cabo and D.A. Sinclair, 2006. Resveratrol improves health and survival of mice on a high-calorie diet. Nature, 444(7117): 337-342. Available from http://www.ncbi.nlm.nih.gov/pubmed/17086191. DOI 10.1038/nature05354.
4. Boissy, P., T.L. Andersen, B.M. Abdallah, M. Kassem, T. Plesner and J.M. Delaisse, 2005. Resveratrol inhibits myeloma cell growth, prevents osteoclast formation, and promotes osteoblast differentiation. Cancer Res, 65(21): 9943-9952. Available from http://www.ncbi.nlm.nih.gov/pubmed/16267019. DOI 10.1158/0008-5472.CAN-05-0651.
5. Cheng, H.L., R. Mostoslavsky, S. Saito, J.P. Manis, Y. Gu, P. Patel, R. Bronson, E. Appella, F.W. Alt and K.F. Chua, 2003. Developmental defects and p53 hyperacetylation in sir2 homolog (sirt1)-deficient mice. Proc Natl Acad Sci U S A, 100(19): 10794-10799. Available from http://www.ncbi.nlm.nih.gov/pubmed/12960381. DOI 10.1073/pnas.1934713100.
6. Dali-Youcef, N., M. Lagouge, S. Froelich, C. Koehl, K. Schoonjans and J. Auwerx, 2007. Sirtuins: The 'magnificent seven', function, metabolism and longevity. Ann Med, 39(5): 335-345. Available from http://www.ncbi.nlm.nih.gov/pubmed/17701476. DOI 10.1080/07853890701408194.
7. Edwards, J.R., D.S. Perrien, N. Fleming, J.S. Nyman, K. Ono, L. Connelly, M.M. Moore, S.T. Lwin, F.E. Yull, G.R. Mundy and F. Elefteriou, 2013. Silent information regulator (sir)t1 inhibits nf-kappab signaling to maintain normal skeletal remodeling. J Bone Miner Res, 28(4): 960-969. Available from http://www.ncbi.nlm.nih.gov/pubmed/23172686. DOI 10.1002/jbmr.1824.
8. Feige, J.N., M. Lagouge, C. Canto, A. Strehle, S.M. Houten, J.C. Milne, P.D. Lambert, C. Mataki, P.J. Elliott and J. Auwerx, 2008. Specific sirt1 activation mimics low energy levels and protects against diet-induced metabolic disorders by enhancing fat oxidation. Cell Metab, 8(5): 347-358. Available from http://www.ncbi.nlm.nih.gov/pubmed/19046567. DOI 10.1016/j.cmet.2008.08.017.
9. Feng, X. and J.M. McDonald, 2011. Disorders of bone remodeling. Annu Rev Pathol, 6: 121-145. Available from http://www.ncbi.nlm.nih.gov/pubmed/20936937. DOI 10.1146/annurev-pathol-011110-130203.
10. Feng, Y.L., X.T. Jiang, F.F. Ma, J. Han and X.L. Tang, 2018. Resveratrol prevents osteoporosis by upregulating foxo1 transcriptional activity. Int J Mol Med, 41(1): 202-212. Available from http://www.ncbi.nlm.nih.gov/pubmed/29115382. DOI 10.3892/ijmm.2017.3208.
11. Gurt, I., H. Artsi, E. Cohen-Kfir, G. Hamdani, G. Ben-Shalom, B. Feinstein, M. El-Haj and R. Dresner-Pollak, 2015. The sirt1 activators srt2183 and srt3025 inhibit rankl-induced osteoclastogenesis in bone marrow-derived macrophages and down-regulate sirt3 in sirt1 null cells. PLoS One, 10(7): e0134391. Available from http://www.ncbi.nlm.nih.gov/pubmed/26226624. DOI 10.1371/journal.pone.0134391.
12. He, X., G. Andersson, U. Lindgren and Y. Li, 2010. Resveratrol prevents rankl-induced osteoclast differentiation of murine osteoclast progenitor raw 264.7 cells through inhibition of ros production.

Biochem Biophys Res Commun, 401(3): 356-362. Available from http://www.ncbi.nlm.nih.gov/pubmed/20851107. DOI 10.1016/j.bbrc.2010.09.053.

13. Howitz, K.T., K.J. Bitterman, H.Y. Cohen, D.W. Lamming, S. Lavu, J.G. Wood, R.E. Zipkin, P. Chung, A. Kisielewski, L.L. Zhang, B. Scherer and D.A. Sinclair, 2003. Small molecule activators of sirtuins extend saccharomyces cerevisiae lifespan. Nature, 425(6954): 191-196. Available from http://www.ncbi.nlm.nih.gov/pubmed/12939617. DOI 10.1038/nature01960.
14. Hubbard, B.P., A.P. Gomes, H. Dai, J. Li, A.W. Case, T. Considine, T.V. Riera, J.E. Lee, S.Y. E, D.W. Lamming, B.L. Pentelute, E.R. Schuman, L.A. Stevens, A.J. Ling, S.M. Armour, S. Michan, H. Zhao, Y. Jiang, S.M. Sweitzer, C.A. Blum, J.S. Disch, P.Y. Ng, K.T. Howitz, A.P. Rolo, Y. Hamuro, J. Moss, R.B. Perni, J.L. Ellis, G.P. Vlasuk and D.A. Sinclair, 2013. Evidence for a common mechanism of sirt1 regulation by allosteric activators. Science, 339(6124): 1216-1219. Available from http://www.ncbi.nlm.nih.gov/pubmed/23471411. DOI 10.1126/science.1231097.
15. Huber, J.L., M.W. McBurney, P.S. Distefano and T. McDonagh, 2010. Sirt1-independent mechanisms of the putative sirtuin enzyme activators srt1720 and srt2183. Future Med Chem, 2(12): 1751-1759. Available from http://www.ncbi.nlm.nih.gov/pubmed/21428798. DOI 10.4155/fmc.10.257.
16. Kim, H.N., L. Han, S. Iyer, R. de Cabo, H. Zhao, C.A. O'Brien, S.C. Manolagas and M. Almeida, 2015. Sirtuin1 suppresses osteoclastogenesis by deacetylating foxos. Mol Endocrinol, 29(10): 1498-1509. Available from http://www.ncbi.nlm.nih.gov/pubmed/26287518. DOI 10.1210/me.2015-1133.
17. Lan, F., K.A. Weikel, J.M. Cacicedo and Y. Ido, 2017. Resveratrol-induced amp-activated protein kinase activation is cell-type dependent: Lessons from basic research for clinical application. Nutrients, 9(7). Available from http://www.ncbi.nlm.nih.gov/pubmed/28708087. DOI 10.3390/nu9070751.
18. Lowe, C., T. Yoneda, B.F. Boyce, H. Chen, G.R. Mundy and P. Soriano, 1993. Osteopetrosis in src-deficient mice is due to an autonomous defect of osteoclasts. Proc Natl Acad Sci U S A, 90(10): 4485-4489. Available from http://www.ncbi.nlm.nih.gov/pubmed/7685105. DOI 10.1073/pnas.90.10.4485.
19. Mercken, E.M., S.J. Mitchell, A. Martin-Montalvo, R.K. Minor, M. Almeida, A.P. Gomes, M. Scheibye-Knudsen, H.H. Palacios, J.J. Licata, Y. Zhang, K.G. Becker, H. Khraiwesh, J.A. Gonzalez-Reyes, J.M. Villalba, J.A. Baur, P. Elliott, C. Westphal, G.P. Vlasuk, J.L. Ellis, D.A. Sinclair, M. Bernier and R. de Cabo, 2014. Srt2104 extends survival of male mice on a standard diet and preserves bone and muscle mass. Aging Cell, 13(5): 787-796. Available from http://www.ncbi.nlm.nih.gov/pubmed/24931715. DOI 10.1111/acel.12220.
20. Milne, J.C., P.D. Lambert, S. Schenk, D.P. Carney, J.J. Smith, D.J. Gagne, L. Jin, O. Boss, R.B. Perni, C.B. Vu, J.E. Bemis, R. Xie, J.S. Disch, P.Y. Ng, J.J. Nunes, A.V. Lynch, H. Yang, H. Galonek, K. Israelian, W. Choy, A. Iffland, S. Lavu, O. Medvedik, D.A. Sinclair, J.M. Olefsky, M.R. Jirousek, P.J. Elliott and C.H. Westphal, 2007. Small molecule activators of sirt1 as therapeutics for the treatment of type 2 diabetes. Nature, 450(7170): 712-716. Available from http://www.ncbi.nlm.nih.gov/pubmed/18046409. DOI 10.1038/nature06261.

21. Mitchell, S.J., A. Martin-Montalvo, E.M. Mercken, H.H. Palacios, T.M. Ward, G. Abulwerdi, R.K. Minor, G.P. Vlasuk, J.L. Ellis, D.A. Sinclair, J. Dawson, D.B. Allison, Y. Zhang, K.G. Becker, M. Bernier and R. de Cabo, 2014. The sirt1 activator srt1720 extends lifespan and improves health of mice fed a standard diet. Cell Rep, 6(5): 836-843. Available from http://www.ncbi.nlm.nih.gov/pubmed/24582957. DOI 10.1016/j.celrep.2014.01.031.
22. Pacholec, M., J.E. Bleasdale, B. Chrunyk, D. Cunningham, D. Flynn, R.S. Garofalo, D. Griffith, M. Griffor, P. Loulakis, B. Pabst, X. Qiu, B. Stockman, V. Thanabal, A. Varghese, J. Ward, J. Withka and K. Ahn, 2010. Srt1720, srt2183, srt1460, and resveratrol are not direct activators of sirt1. J Biol Chem, 285(11): 8340-8351. Available from http://www.ncbi.nlm.nih.gov/pubmed/20061378. DOI 10.1074/jbc.M109.088682.
23. Pearson, K.J., J.A. Baur, K.N. Lewis, L. Peshkin, N.L. Price, N. Labinskyy, W.R. Swindell, D. Kamara, R.K. Minor, E. Perez, H.A. Jamieson, Y. Zhang, S.R. Dunn, K. Sharma, N. Pleshko, L.A. Woollett, A. Csiszar, Y. Ikeno, D. Le Couteur, P.J. Elliott, K.G. Becker, P. Navas, D.K. Ingram, N.S. Wolf, Z. Ungvari, D.A. Sinclair and R. de Cabo, 2008. Resveratrol delays age-related deterioration and mimics transcriptional aspects of dietary restriction without extending life span. Cell Metab, 8(2): 157-168. Available from http://www.ncbi.nlm.nih.gov/pubmed/18599363. DOI 10.1016/j.cmet.2008.06.011.
24. Price, N.L., A.P. Gomes, A.J. Ling, F.V. Duarte, A. Martin-Montalvo, B.J. North, B. Agarwal, L. Ye, G. Ramadori, J.S. Teodoro, B.P. Hubbard, A.T. Varela, J.G. Davis, B. Varamini, A. Hafner, R. Moaddel, A.P. Rolo, R. Coppari, C.M. Palmeira, R. de Cabo, J.A. Baur and D.A. Sinclair, 2012. Sirt1 is required for ampk activation and the beneficial effects of resveratrol on mitochondrial function. Cell Metab, 15(5): 675-690. Available from http://www.ncbi.nlm.nih.gov/pubmed/22560220. DOI 10.1016/j.cmet.2012.04.003.
25. Rogina, B. and S.L. Helfand, 2004. Sir2 mediates longevity in the fly through a pathway related to calorie restriction. Proc Natl Acad Sci U S A, 101(45): 15998-16003. Available from http://www.ncbi.nlm.nih.gov/pubmed/15520384. DOI 10.1073/pnas.0404184101.
26. Saltel, F., A. Chabadel, E. Bonnelye and P. Jurdic, 2008. Actin cytoskeletal organisation in osteoclasts: A model to decipher transmigration and matrix degradation. Eur J Cell Biol, 87(8-9): 459-468. Available from http://www.ncbi.nlm.nih.gov/pubmed/18294724. DOI 10.1016/j.ejcb.2008.01.001.
27. Satoh, A., C.S. Brace, N. Rensing, P. Cliften, D.F. Wozniak, E.D. Herzog, K.A. Yamada and S. Imai, 2013. Sirt1 extends life span and delays aging in mice through the regulation of nk2 homeobox 1 in the dmh and lh. Cell Metab, 18(3): 416-430. Available from http://www.ncbi.nlm.nih.gov/pubmed/24011076. DOI 10.1016/j.cmet.2013.07.013.
28. Schneider, C.A., W.S. Rasband and K.W. Eliceiri, 2012. Nih image to imagej: 25 years of image analysis. Nat Methods, 9(7): 671-675. Available from http://www.ncbi.nlm.nih.gov/pubmed/22930834.
29. Shakibaei, M., C. Buhrmann and A. Mobasheri, 2011. Resveratrol-mediated sirt-1 interactions with p300 modulate receptor activator of nf-kappab ligand (rankl) activation of nf-kappab signaling and inhibit osteoclastogenesis in bone-derived cells. J Biol Chem, 286(13): 11492-11505. Available from http://www.ncbi.nlm.nih.gov/pubmed/21239502. DOI 10.1074/jbc.M110.198713.

30. Smith, J.J., R.D. Kenney, D.J. Gagne, B.P. Frushour, W. Ladd, H.L. Galonek, K. Israelian, J. Song, G. Razvadauskaite, A.V. Lynch, D.P. Carney, R.J. Johnson, S. Lavu, A. Iffland, P.J. Elliott, P.D. Lambert, K.O. Elliston, M.R. Jirousek, J.C. Milne and O. Boss, 2009. Small molecule activators of sirt1 replicate signaling pathways triggered by calorie restriction in vivo. BMC Syst Biol, 3: 31. Available from http://www.ncbi.nlm.nih.gov/pubmed/19284563. DOI 10.1186/1752-0509-3-31.
31. Soriano, P., C. Montgomery, R. Geske and A. Bradley, 1991. Targeted disruption of the c-src proto-oncogene leads to osteopetrosis in mice. Cell, 64(4): 693-702. Available from http://www.ncbi.nlm.nih.gov/pubmed/1997203.
32. Wang, X., L. Chen and W. Peng, 2017. Protective effects of resveratrol on osteoporosis via activation of the sirt1-nf-kappab signaling pathway in rats. Exp Ther Med, 14(5): 5032-5038. Available from http://www.ncbi.nlm.nih.gov/pubmed/29201210. DOI 10.3892/etm.2017.5147.
33. Wood, J.G., B. Rogina, S. Lavu, K. Howitz, S.L. Helfand, M. Tatar and D. Sinclair, 2004. Sirtuin activators mimic caloric restriction and delay ageing in metazoans. Nature, 430(7000): 686-689. Available from http://www.ncbi.nlm.nih.gov/pubmed/15254550. DOI 10.1038/nature02789.
34. Yamazaki, Y., I. Usui, Y. Kanatani, Y. Matsuya, K. Tsuneyama, S. Fujisaka, A. Bukhari, H. Suzuki, S. Senda, S. Imanishi, K. Hirata, M. Ishiki, R. Hayashi, M. Urakaze, H. Nemoto, M. Kobayashi and K. Tobe, 2009. Treatment with srt1720, a sirt1 activator, ameliorates fatty liver with reduced expression of lipogenic enzymes in msg mice. Am J Physiol Endocrinol Metab, 297(5): E1179-1186. Available from http://www.ncbi.nlm.nih.gov/pubmed/19724016. DOI 10.1152/ajpendo.90997.2008.
35. Zainabadi, K., C.J. Liu, A.L.M. Caldwell and L. Guarente, 2017. Sirt1 is a positive regulator of in vivo bone mass and a therapeutic target for osteoporosis. PLoS One, 12(9): e0185236. Available from http://www.ncbi.nlm.nih.gov/pubmed/28937996. DOI 10.1371/journal.pone.0185236.

Figures

Fig 1

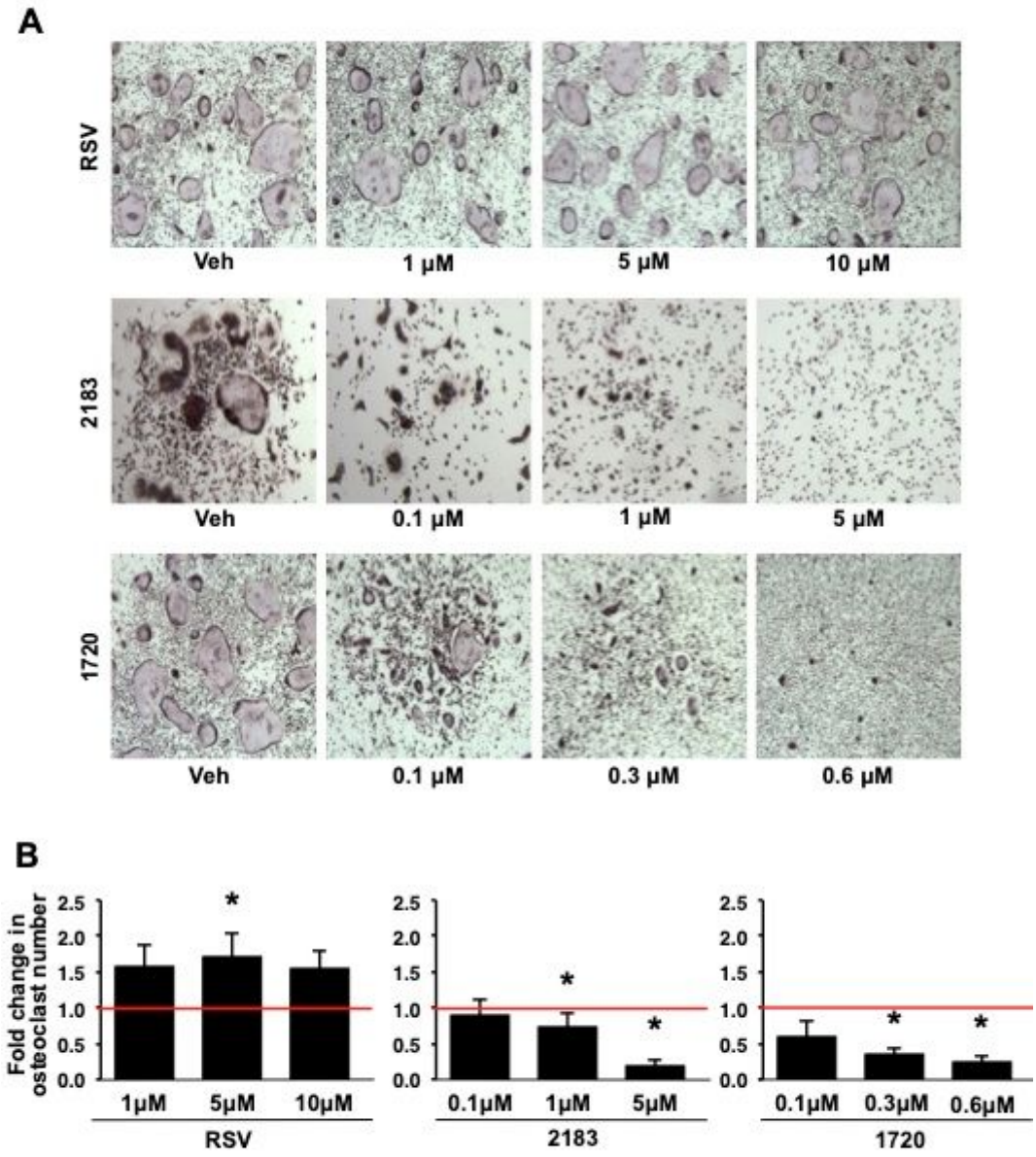

Figure 1

SRT2183 and SRT1720 inhibit osteoclast formation, while RSV does not (a) TRAP staining of RSV, SRT2183 and SRT1720 treated multi-nuclear osteoclasts in the presence of M-CSF (20 ng/ml) and RANKL (40 ng/ml). (b) Osteoclasts with 3 or more nuclei were counted, and the values are represented in fold change as compared to vehicle control (red line). Three independent experiments were performed with ≥ 3 wells per condition. * $p < 0.05$, compared with WT vehicle control. Data expressed as mean ± SD.

Fig 1

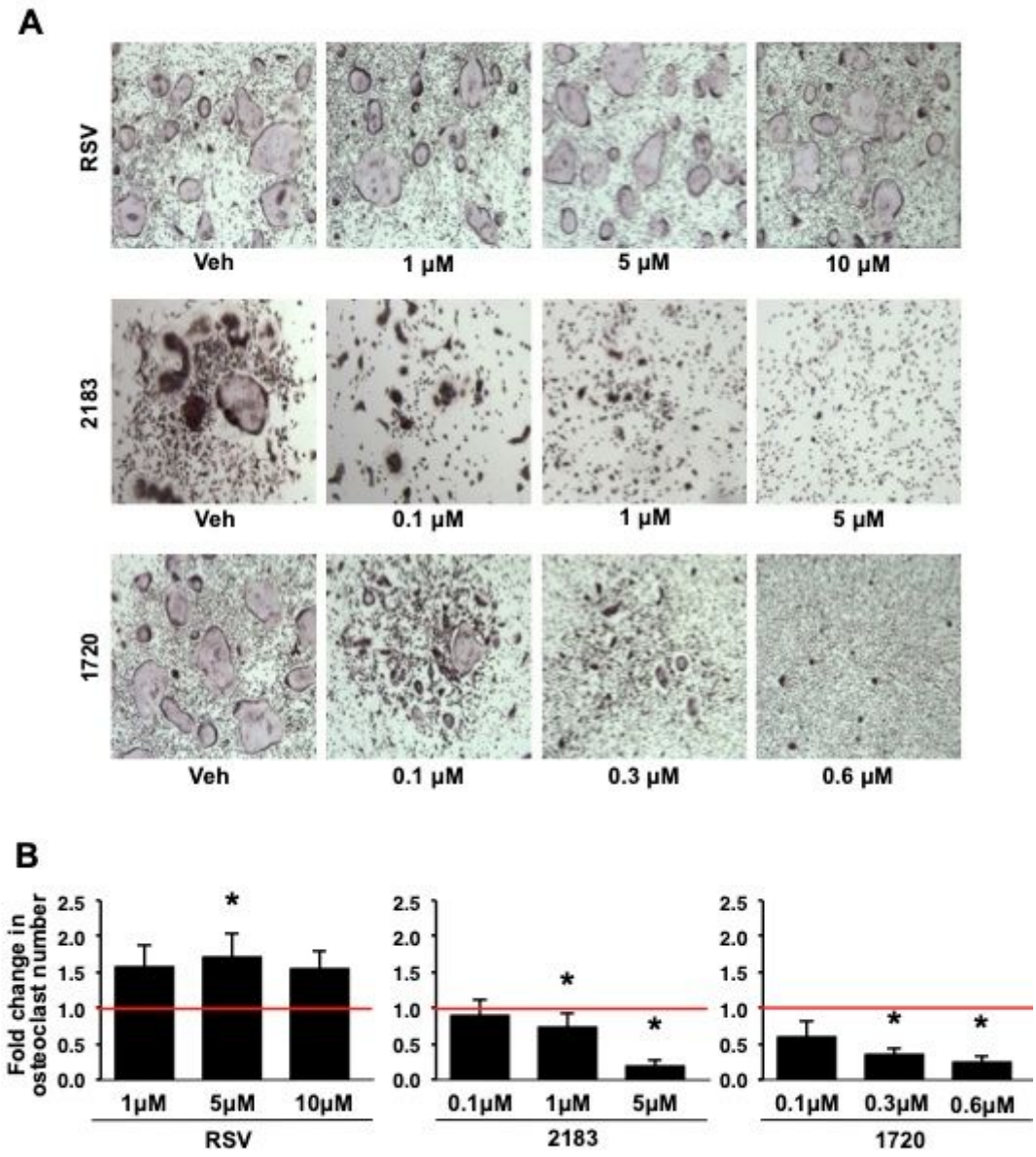

Figure 1

SRT2183 and SRT1720 inhibit osteoclast formation, while RSV does not (a) TRAP staining of RSV, SRT2183 and SRT1720 treated multi-nuclear osteoclasts in the presence of M-CSF (20 ng/ml) and RANKL (40 ng/ml). (b) Osteoclasts with 3 or more nuclei were counted, and the values are represented in fold change as compared to vehicle control (red line). Three independent experiments were performed with ≥ 3 wells per condition. * $p < 0.05$, compared with WT vehicle control. Data expressed as mean ± SD.

Fig 2

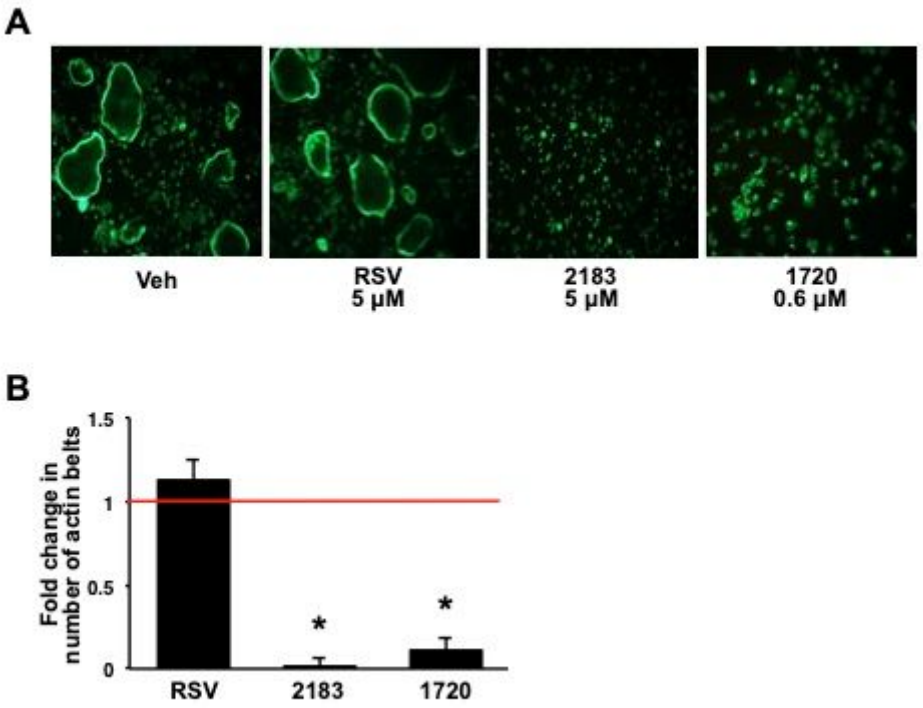

Figure 2

SRT2183 and SRT1720 disrupt actin belt formation, while RSV does not (a) Primary mouse BMCs were treated with 5 μM RSV, 5 μM SRT2183, or 0.6 μM SRT1720 in the presence of M-CSF and RANKL for 6 - 7 days, and then the osteoclasts were fixed and stained with FITC-phalloidin to view actin belts. (b) Complete belt around the perimeter of the osteoclasts were counted. Three independent experiments were performed with ≥ 3 wells per condition. * $p < 0.05$, compared with WT vehicle control. Data expressed as mean ± SD.

Fig 2

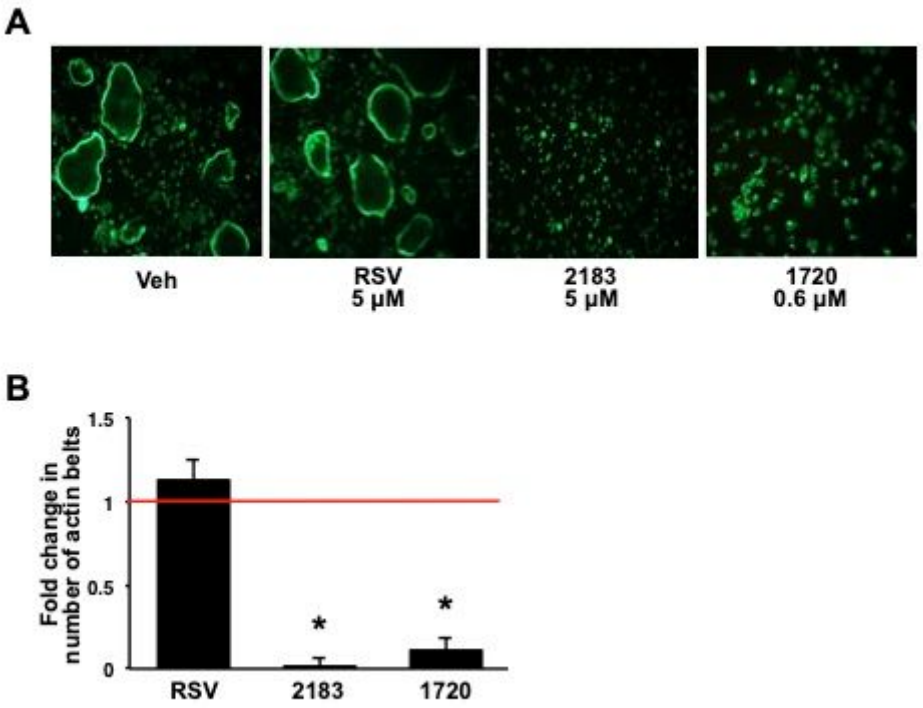

Figure 2

SRT2183 and SRT1720 disrupt actin belt formation, while RSV does not (a) Primary mouse BMCs were treated with 5 μM RSV, 5 μM SRT2183, or 0.6 μM SRT1720 in the presence of M-CSF and RANKL for 6 - 7 days, and then the osteoclasts were fixed and stained with FITC-phalloidin to view actin belts. (b) Complete belt around the perimeter of the osteoclasts were counted. Three independent experiments were performed with ≥ 3 wells per condition. * $p < 0.05$, compared with WT vehicle control. Data expressed as mean ± SD.

Fig 3

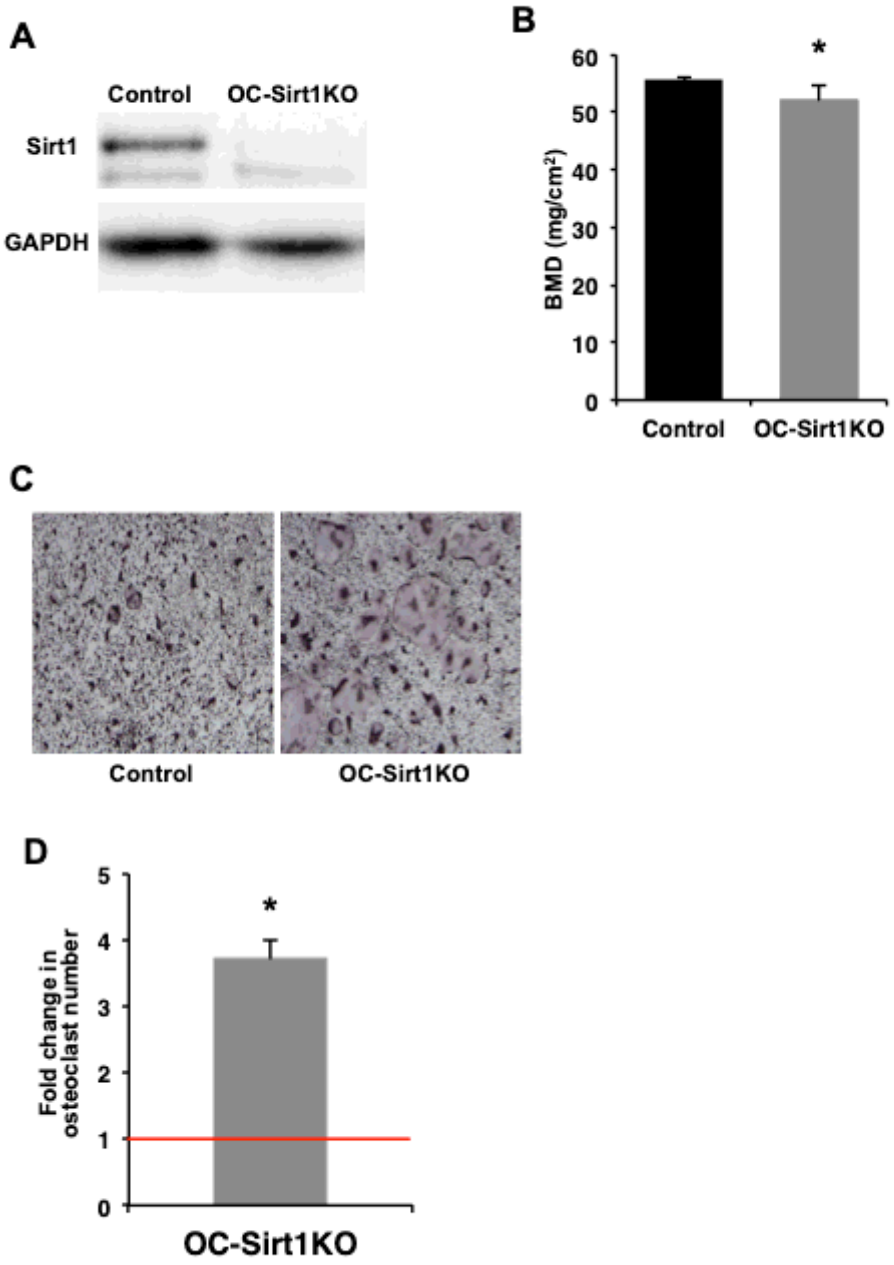

Figure 3

Osteoclast specific Sirt1 knockout (OC-Sirt1KO) mice exhibit low bone mineral density and greater number of osteoclasts ex vivo (a) Western blot analysis of Sirt1 expression in osteoclasts derived from OC-Sirt1KO mice and littermate control mice BMCs (n=3). (b) Bone mineral density of 4-month-old male littermate control and OC Sirt1KO mice were assessed using dual energy X-ray absorptiometry (n=6). (c) BMCs from littermate control and OC-Sirt1KO mice were treated for 6 days in the presence of 20 ng/ml M-CSF and 40 ng/ml RANKL. After 6 days, osteoclasts were fixed and stained for TRAP. (d) Osteoclasts with 3 or more nuclei were counted, and the values are represented in fold change as compared to littermate

control. Three independent experiments were performed with ≥ 3 wells per condition. * p<0.05, compared with littermate control. Data expressed as mean ± SD.

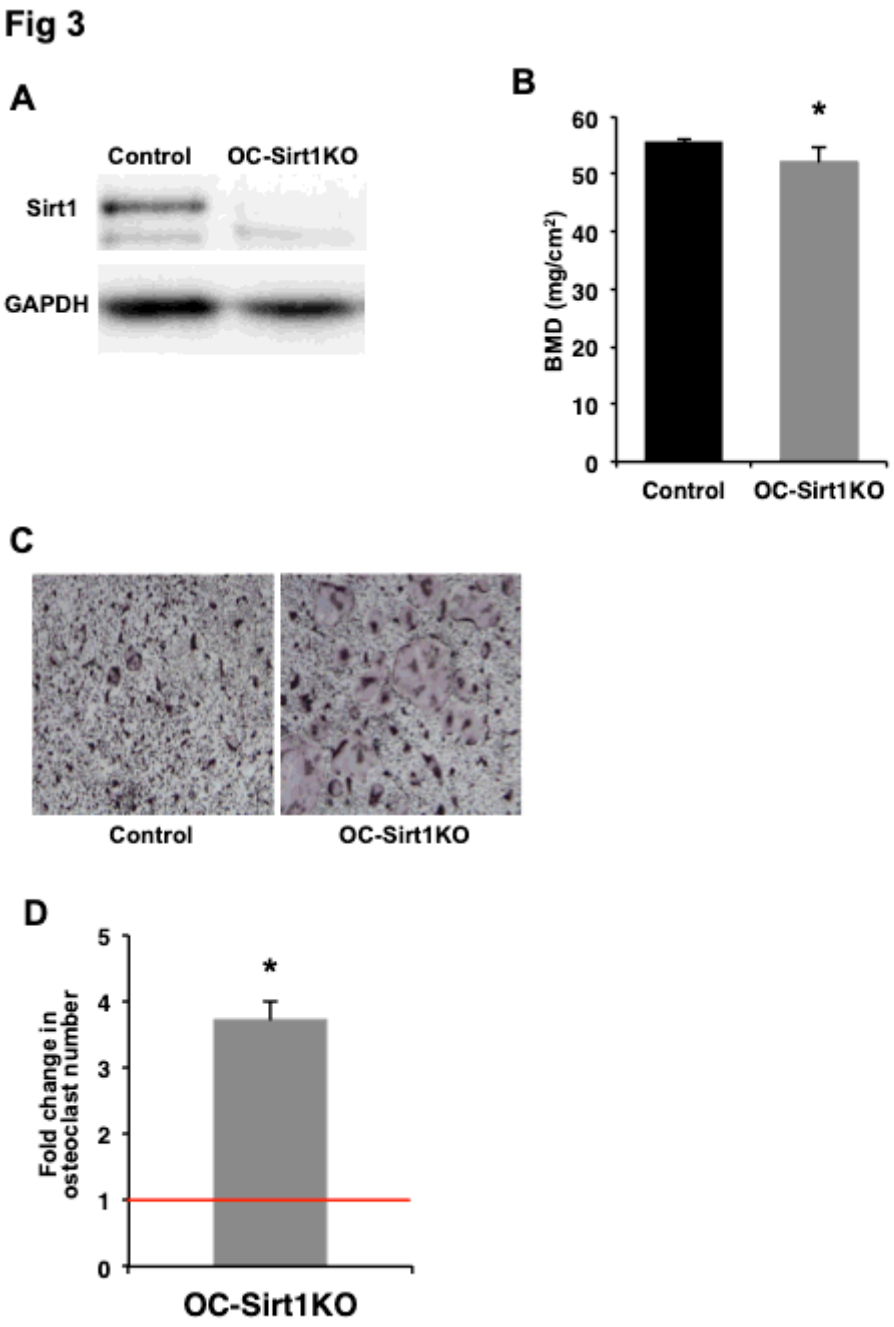

Figure 3

Osteoclast specific Sirt1 knockout (OC-Sirt1KO) mice exhibit low bone mineral density and greater number of osteoclasts ex vivo (a) Western blot analysis of Sirt1 expression in osteoclasts derived from OC-Sirt1KO mice and littermate control mice BMCs (n=3). (b) Bone mineral density of 4-month-old male littermate control and OC Sirt1KO mice were assessed using dual energy X-ray absorptiometry (n=6). (c) BMCs from littermate control and OC-Sirt1KO mice were treated for 6 days in the presence of 20 ng/ml M-CSF and 40 ng/ml RANKL. After 6 days, osteoclasts were fixed and stained for TRAP. (d) Osteoclasts with

3 or more nuclei were counted, and the values are represented in fold change as compared to littermate control. Three independent experiments were performed with ≥ 3 wells per condition. * p<0.05, compared with littermate control. Data expressed as mean ± SD.

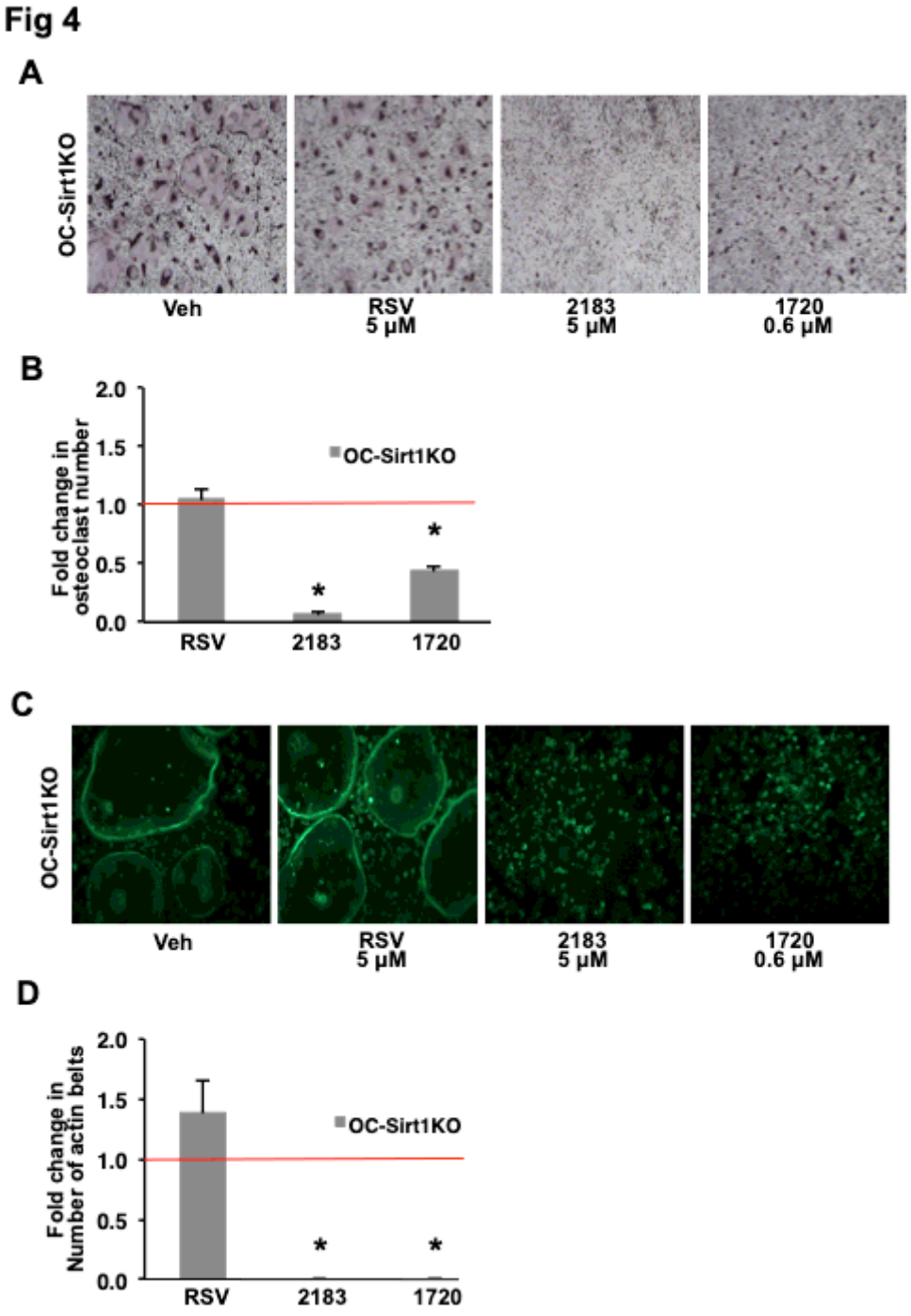

Figure 4

SRT2183 and SRT1720 inhibit osteoclast and actin belt formation in bone marrow cells derived from OC-Sirt1KO mice BMCs from OC-Sirt1KO mice were treated for 6 days with 5 μM RSV, 5 μM SRT2183, or 0.6 μM SRT1720 in the presence of 20 ng/ml M-CSF and 40 ng/ml RANKL. After 6 days, osteoclasts were fixed and stained with TRAP (a) to count osteoclasts with 3 or more nuclei (b) or stained with FITC-

phalloidin (c) to visualize and count actin belts (d). Three independent experiments were performed with ≥ 3 wells per condition. * p<0.05, compared with littermate control. Data expressed as mean ± SD.

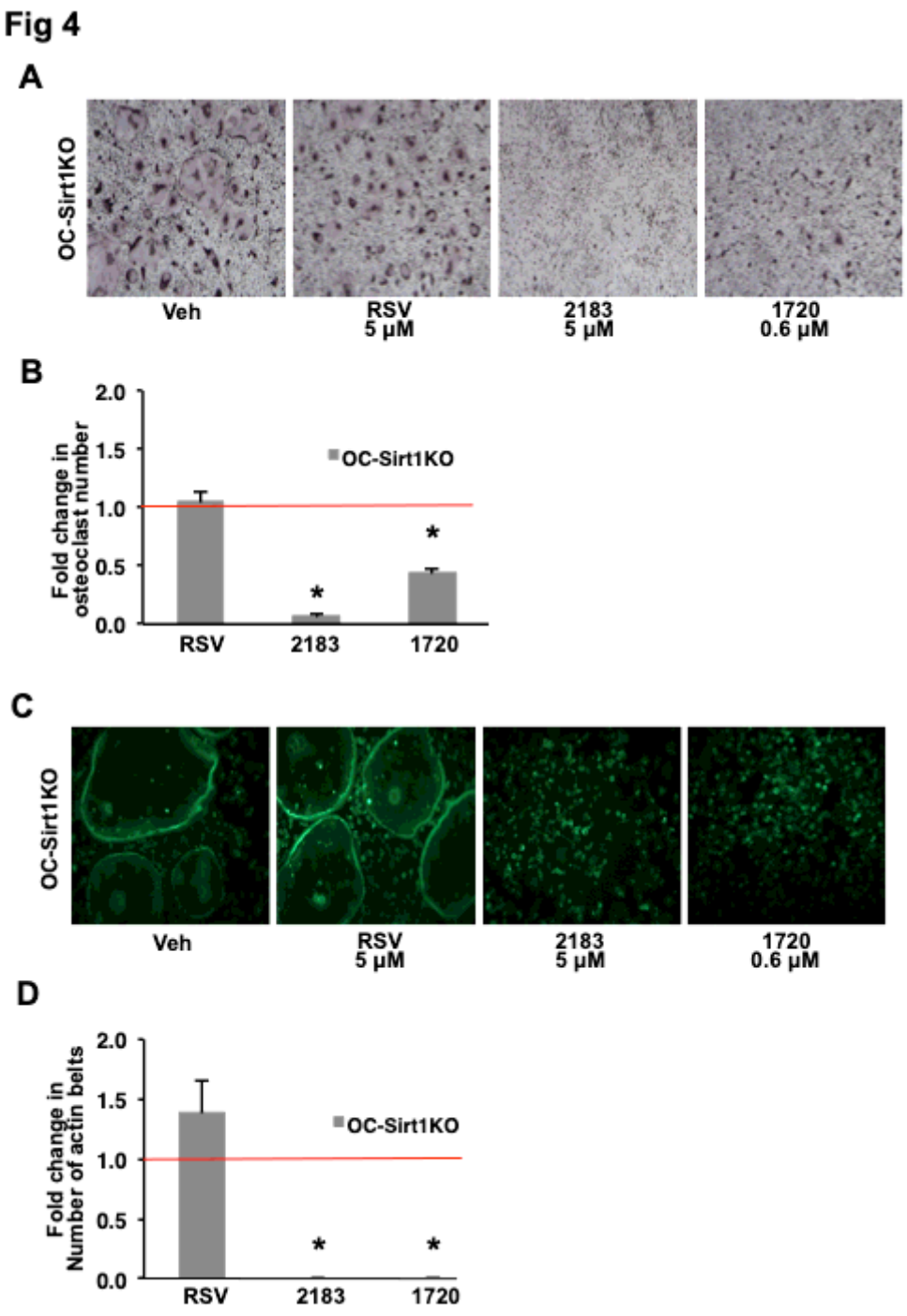

Figure 4

SRT2183 and SRT1720 inhibit osteoclast and actin belt formation in bone marrow cells derived from OC-Sirt1KO mice BMCs from OC-Sirt1KO mice were treated for 6 days with 5 μM RSV, 5 μM SRT2183, or 0.6 μM SRT1720 in the presence of 20 ng/ml M-CSF and 40 ng/ml RANKL. After 6 days, osteoclasts were fixed and stained with TRAP (a) to count osteoclasts with 3 or more nuclei (b) or stained with FITC-phalloidin (c) to visualize and count actin belts (d). Three independent experiments were performed with ≥ 3 wells per condition. * p<0.05, compared with littermate control. Data expressed as mean ± SD.

Fig 5

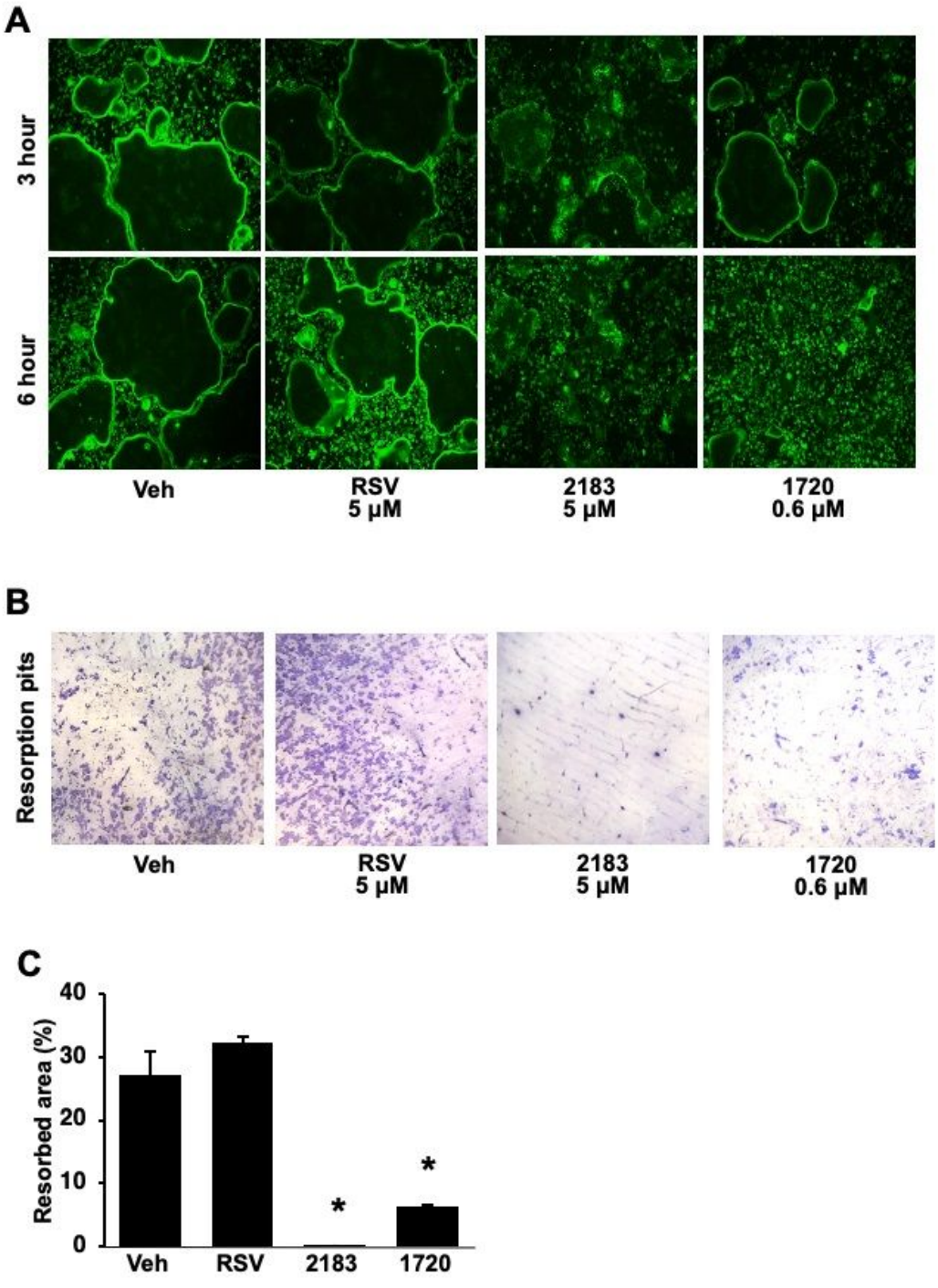

Figure 5

SRT2183 and SRT1720 disrupt actin belts and prevent resorption in mature osteoclasts Multi-nuclear mature osteoclasts were lifted off the plate using accutase solution and reseeded on a tissue culture plate or cortical bovine bone slices. The reseeded mature osteoclasts in the tissue culture plate were treated 3 h and 6 h with 5 μM RSV, 5 μM SRT2183, or 0.6 μM SRT1720, then fixed and stained with FITC-Phalloidin to visualize actin belts (a). Mature osteoclasts reseeded on bone slices were treated for 72 h

and the resorption pits were visualized using 0.1% toluidine blue stain (b). The percentage of eroded area in a given bone slice was assessed using ImageJ software (c). Three independent experiments were performed with ≥ 3 wells per condition. * $p < 0.05$, compared with WT vehicle control. Data expressed as mean ± SD.

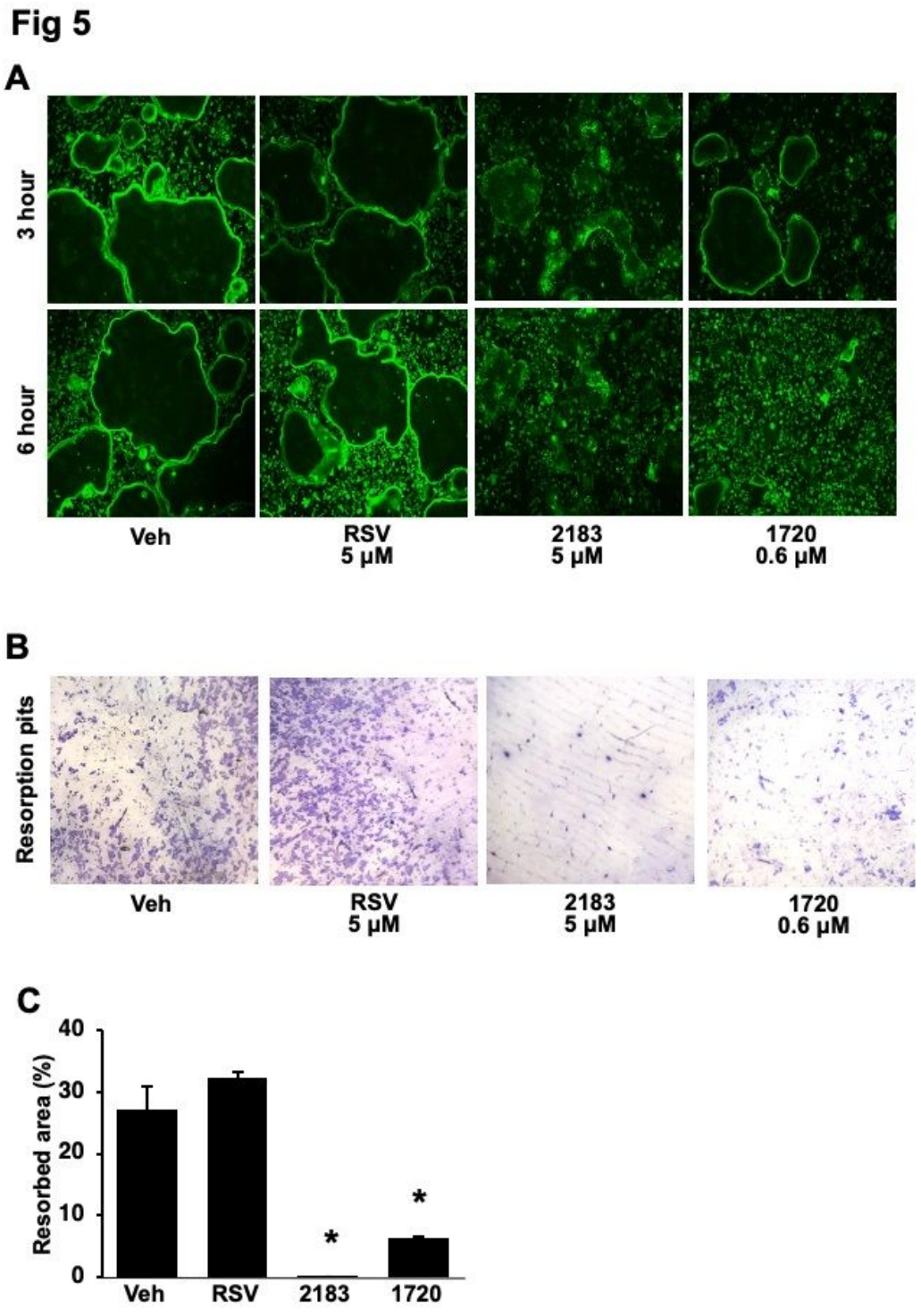

Figure 5

SRT2183 and SRT1720 disrupt actin belts and prevent resorption in mature osteoclasts Multi-nuclear mature osteoclasts were lifted off the plate using accutase solution and reseeded on a tissue culture plate or cortical bovine bone slices. The reseeded mature osteoclasts in the tissue culture plate were treated 3 h and 6 h with 5 μM RSV, 5 μM SRT2183, or 0.6 μM SRT1720, then fixed and stained with FITC-Phalloidin to visualize actin belts (a). Mature osteoclasts reseeded on bone slices were treated for 72 h and the resorption pits were visualized using 0.1% toluidine blue stain (b). The percentage of eroded area in a given bone slice was assessed using ImageJ software (c). Three independent experiments were performed with ≥ 3 wells per condition. * $p < 0.05$, compared with WT vehicle control. Data expressed as mean ± SD.

Supplementary Files

This is a list of supplementary files associated with this preprint. Click to download.

- ARRIVEReportingGuidelinesChecklist.pdf
- ARRIVEReportingGuidelinesChecklist.pdf
- Supp.Fig1.tiff
- Supp.Fig1.tiff
- Supp.Fig2.tiff
- Supp.Fig2.tiff
- Supp.Fig3.tiff
- Supp.Fig3.tiff
- Supp.Fig4.tiff
- Supp.Fig4.tiff
- Supplementarymaterial.docx
- Supplementarymaterial.docx
- ThiyagarajanSTACsInVitrodata.xlsx
- ThiyagarajanSTACsInVitrodata.xlsx
- Westernblotfullimage.pdf
- Westernblotfullimage.pdf